

Influence of Strains and Defects on Ferroelectric and Dielectric Properties of Thin-Film Barium–Strontium Titanates

Davor BALZAR^{1,2,*}, Padmanabhan A. RAMAKRISHNAN³, Priscila SPAGNOL⁴,
 Sugantha MANI^{1,2}, Allen M. HERMANN³ and Mohammad A. MATIN⁵

¹Department of Physics & Astronomy, University of Denver, Denver, CO 80208, U.S.A.

²National Institute of Standards and Technology, Boulder, CO 80305, U.S.A.

³Department of Physics, University of Colorado, Boulder, CO 80309, U.S.A.

⁴Chemistry Institute, UNESP, CEP 14801-970 Araraquara-SP, Brazil

⁵Department of Engineering, University of Denver, Denver, CO 80208, U.S.A.

(Received May 29, 2002; accepted for publication August 8, 2002)

Pristine, W and Mn 1% doped Ba_{0.6}Sr_{0.4}TiO₃ epitaxial thin films grown on the LaAlO₃ substrate were deposited by pulsed laser deposition (PLD). Dielectric and ferroelectric properties were determined by the capacitance measurements and X-ray diffraction was used to determine both residual elastic strains and defect-related inhomogeneous strains by analyzing diffraction line shifts and line broadening, respectively. We found that both elastic and inhomogeneous strains are affected by doping. This strain correlates with the change in Curie-Weiss temperature and can qualitatively explain changes in dielectric loss. To explain the experimental findings, we model the dielectric and ferroelectric properties of interest in the framework of the Landau-Ginzburg-Devonshire thermodynamic theory. As expected, an elastic-strain contribution due to the epilayer-substrate misfit has an important influence on the free-energy. However, additional terms that correspond to the defect-related inhomogeneous strain had to be introduced to fully explain the measurements. [DOI: 10.1143/JJAP.41.6628]

KEYWORDS: ferroelectric thin films, strain, defects, Curie-Weiss temperature, barium–strontium titanate

1. Introduction

Thin film ferroelectric (FE) materials have received considerable attention because of their growing use in electronic, electro-optical, optical and acoustic devices. Potential applications include integrated, nonvolatile, and dynamic random access memories, pyroelectric detectors, and acoustic transducers.¹⁾ These materials also exhibit nonlinear dielectric properties under an external electric field, which is exploited in tunable microwave devices, such as microstrip line phase shifters, high-Q resonators, and tunable filters.²⁾ For these applications, it is imperative that the films exhibit a high dielectric constant and tunability, and low dielectric loss. While reasonable success has been achieved with tunability, the major challenge has been lowering the dielectric loss and in particular understanding its mechanism. It was elucidated that losses depend on substrate and post annealing treatments³⁾ and the film thickness,⁴⁾ in that the free-standing films generally have low losses⁵⁾ and that crystalline SrRuO₃, YBCO⁶⁾ and amorphous⁷⁾ buffer layers decrease losses. This indicates that minimizing lattice misfit between the film and substrate is of utmost importance. Indeed, dielectric losses depend on residual stresses of both intrinsic (caused by optical-phonon interaction with the applied electric field) and extrinsic (caused by lattice defects) nature. The latter is an especially important and complicated process because many possible defects can be involved, such as ferroelectric domains, grain boundaries, stacking faults, dislocations, vacancies, and vacancy complexes. Of the various ferroelectric materials, perovskite oxide thin films are considered as potential candidates for tunable microwave devices because of their high dielectric constant. Materials investigated widely are based on solid solutions of Ba_xSr_{1-x}TiO₃ (BSTO), which exhibit high tunability and easily controlled Curie temperature by varying chemical

composition. Losses can be controlled by doping very small percentages (< 4%) of ions such as Mn, W, Ca, Mg, and Zr.⁸⁾

Our previous studies on doped BSTO films⁹⁾ indicate that the ferroelectric transition temperature and the extrinsic dielectric losses depend on the internal stresses and defects. Thus it is evident that lattice strain plays a crucial role in influencing the dielectric and ferroelectric properties. To understand this further, we attempted to investigate the effect of doping on the ferroelectric properties. Here, we report on the correlation between Curie-Weiss temperature and residual elastic strain (stress) and defect concentration.

2. Theory

A comprehensive treatment of the influence of homogeneous strain, due to the misfit in lattice parameter and thermal expansion coefficients, on the ferroelectric transition temperature and electrical permittivity, was reported by Pertsev *et al.*¹⁰⁾ They start with the expression for the Gibbs free energy, close to the transition temperature and appearance of polarization P :

$$\begin{aligned}
 G = & a_1(P_1^2 + P_2^2 + P_3^2) + a_{11}(P_1^4 + P_2^4 + P_3^4) \\
 & + a_{12}(P_1^2 P_2^2 + P_1^2 P_3^2 + P_2^2 P_3^2) + a_{111}(P_1^6 + P_2^6 + P_3^6) \\
 & + a_{112}[P_1^4(P_2^2 + P_3^2) + P_3^4(P_1^2 + P_2^2) + P_2^4(P_1^2 + P_3^2)] \\
 & + a_{123}P_1^2 P_2^2 P_3^2 - Q_{11}(\sigma_1 P_1^2 + \sigma_2 P_2^2) \\
 & - Q_{12}[\sigma_1(P_2^2 + P_3^2) + \sigma_2(P_1^2 + P_3^2)] - Q_{44}P_1 P_2 \sigma_6 \\
 & - 1/2s_{11}(\sigma_1^2 + \sigma_2^2) - s_{12}\sigma_1\sigma_2 - 1/2s_{44}\sigma_6^2.
 \end{aligned}$$

Here, $a_{i,j,k}$ are dielectric stiffness coefficients, s_{ij} is the elastic compliance tensor, Q_{ij} the electrostrictive tensor, and σ_i is the mechanical stress tensor, all in the Voigt condensed tensor notation.

In the approximation of the single-domain two-dimensional

*E-mail address: balzar@du.edu

thin film constrained by the substrate, one can write the additional term to the Gibbs free energy due to elastic-strain e_i contribution as:¹⁰⁾

$$G' = G + \sum_i e_i \sigma_i.$$

This expression considers only elastic strains. However, crystalline defects (oxygen vacancies, for instance) will affect the polarization of a ferroelectric.¹¹⁾ We proposed¹²⁾ that the internal crystalline defects induce similar changes of the Gibbs free energy,

$$G'' = G' + \sum_i \varepsilon_i \Sigma_i,$$

$$\Delta T_{C-W} = \max \left\{ 2C \varepsilon_0 \left(\frac{2Q_{12}}{s_{11} + s_{12}} e_m + \frac{Q_{11} + 2Q_{12}}{s_{11} + 2s_{12}} \varepsilon_m \right), 2C \varepsilon_0 \left(\frac{Q_{11} + Q_{12}}{s_{11} + s_{12}} e_m + \frac{Q_{11} + 2Q_{12}}{s_{11} + 2s_{12}} \varepsilon_m \right) \right\}. \quad (2)$$

Here, C and ε_0 are the Curie-Weiss constant and the permittivity of the vacuum, respectively. The second term in eq. (2) is given by the inhomogeneous strain. Note that its contribution is always positive unlike that of the elastic-strain term that can be either positive or negative, depending on whether the film is in tension or compression parallel to its surface.

3. Experimental

The pristine BSTO and Mn, W-doped and co-doped $\text{Ba}_{0.6}\text{Sr}_{0.4}\text{Ti}_{0.99}\text{M}_{0.01}\text{O}_3$ ($M = \text{Mn, W}$) thin films were deposited on (001) LaAlO_3 (LAO) substrate using a KrF excimer laser (248 nm) at 700°C at oxygen partial pressures of 300 mTorr. During deposition, the stoichiometric BSTO targets with densities of 98% were used. The energy density was about 1.5–2 J/cm². The films were post-annealed in flowing oxygen at 950°C for 6 h.

Dielectric measurements were carried out on these films using a 4-capacitor shadow mask design with interdigitated capacitors. The mask has 6 terminal pads for contact, with finger widths of 125 μm and finger separation of 75 μm . The interdigitated capacitor configurations were obtained by thermal evaporation of silver to a thickness of 150 nm. Fine-gauge copper leads were then attached to each capacitor using silver paste. The whole assembly was then annealed at 300°C in Ar to ensure good electrical contact and to decompose the organic matter present in the silver paste.

The capacitance and dielectric loss ($\tan \delta$) were measured using a HP 4192A LCR meter¹³⁾ at a constant frequency of 1 MHz. For temperature variation a closed cycle He refrigerator was used. Automated data acquisition was achieved by the LABVIEW¹³⁾ program. A standard 2 pF capacitor was used to calibrate the instrument which gave < 1% error in the frequency range studied.

The optical properties were measured with a dual mode automatic ellipsometer model L116A¹³⁾ at room temperature. The ellipsometer measurements can be used for determining the film thickness and refractive index of optically transparent and absorbing layers, in the range between a few Å and a few μm . The film thickness was relatively nonuniform due to the deposition technique used and varied in the range of 1000–3500 Å.

through the inhomogeneous strain ε_i (so-called strain of the III kind that influences the diffraction line width, for instance) and the stress of the III kind Σ_i .

On the assumption that the spontaneous polarization axis is perpendicular to the film surface and isotropy of inhomogeneous strain, we have:¹²⁾

$$G'' = a_3^* P_3^2 + a_{33}^* P_3^4 + a_{111} P_3^6 + \frac{e_m^2}{s_{11} + s_{12}} + \frac{3}{2} \frac{\varepsilon_m^2}{s_{11} + 2s_{12}} \quad (1)$$

where the renormalized coefficients a^* were given elsewhere.¹²⁾ Similarly, the Curie-Weiss temperature is renormalized:¹²⁾

X-ray diffraction (XRD) data were collected using commercial four-circle and two-circle double-axis diffractometers with Cu $K\alpha$ radiation excited at 45 kV and 40 mA. To thoroughly study the misfit relationship at the film-substrate interface, we recorded reciprocal space maps for all films. Reciprocal space maps discern differences between different types of defects in epilayers, in particular mosaicity parallel to the film surface and strain variations perpendicular to the film surface. Reciprocal space maps of asymmetric reflections (013) were used to obtain both parallel and perpendicular (to the film surface) lattice parameters. All films showed relatively small broadening of various amounts, as compared to the substrate. Broadening was evident both parallel to the surface, thus indicating somewhat increased mosaicity, and perpendicular to it, which could be caused by small correlation lengths, inhomogeneous strain, and the through-depth stoichiometry variations. To investigate this point further, we conducted a careful study of line broadening perpendicular to the film surface. The analysis takes into consideration multiple Bragg reflections, thus allowing for an unequivocal separation of correlation-length and inhomogeneous-strain effects on line broadening.¹⁴⁾ Our experimental setup was a low resolution one without the incident-beam (Bartels) monochromator. To account for wavelength dispersion, we corrected the measured profiles for effects of instrumental broadening. This correction was accomplished by measurements of line profiles of the bare LAO substrate reflections and also includes corrections for additional instrumental effects.¹⁴⁾

4. Results and discussion

Figure 1 shows a plot of relative permittivity and dielectric loss ($\tan \delta$), measured at 1 MHz frequency with both zero and 35 V bias in order to estimate tunability, as a function of temperature for the pristine BSTO thin film. Relative permittivity shows a relatively broad ferroelectric transition around room temperature. The temperature at the curve maximum was taken as a ferroelectric transition temperature T_{C-W} . Because the measurements were taken at a frequency lower than the microwave region, we do not discuss the influence of strains and defects on dielectric loss and relative permittivity here.

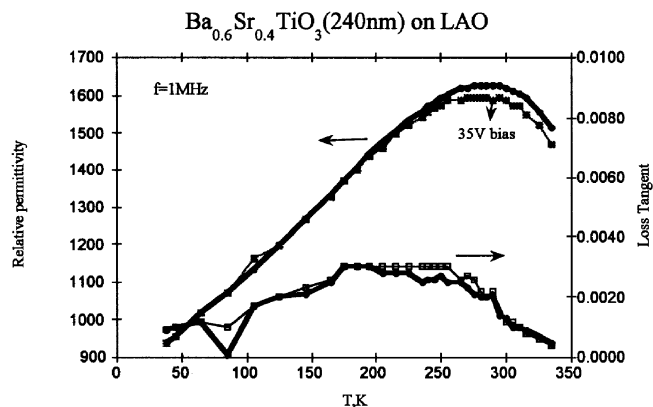


Fig. 1. Dielectric permittivity and loss, measured at 1 MHz frequency at zero and 35 V bias, as a function of temperature for undoped Ba_{0.60}Sr_{0.40}TiO₃ thin film on the LaAlO₃ substrate.

XRD measurements were used to confirm the epitaxial relationship between the films and substrate and to calculate lattice parameters. Coupled $\theta/2\theta$ scans perpendicular to the surface showed only 00 l Bragg reflections for all films that confirm preferential [001] growth perpendicular to the surface. A good BSTO [001] || LAO (pseudo) [001] epitaxy with the substrate was confirmed by the scans parallel to the film surface (ϕ scans), which showed four maxima 90° apart for all the films. Figures 2(a) and 2(b) show the $\theta/2\theta$ and ϕ scans for the pristine BSTO film.

At room temperature, there is a large misfit (up to 5%) between the (pseudocubic) lattice parameter of the substrate and that of the epilayer. Such a large difference is accommodated through the introduction of misfit dislocations mainly at the growth temperature. An incomplete misfit relaxation at growing temperature and different thermal expansion coefficients of the film and substrate may cause tetragonal distortion of the film, although the bulk BSTO with this composition is cubic at room temperature. For our thin films, the epilayer dimension parallel to the epilayer-substrate interface (designated as a) stayed in compression and that perpendicular to it, in tension (designated as c). If the “relaxed” cubic lattice parameter of an epilayer is defined as

$$a^R = \frac{c + 2a(v/(1 - v))}{1 + 2v/(1 - v)}$$

where v is the Poisson ratio (approximately taken as 1/3), the relaxed lattice parameter is estimated to be the same for all the samples within the single standard uncertainty. The value, $a = 3.957(6) \text{ \AA}$ is slightly lower than the value for bulk BSTO reported in the literature, $a = 3.965 \text{ \AA}$.¹⁵⁾ It may indicate that the actual stoichiometry of the thin films, which we did not measure, is richer in Sr than the nominal target composition.

From the values of relaxed and measured lattice parameters, we calculated elastic strains:

$$e_a = a/a^R - 1; \quad e_c = c/a^R - 1.$$

They are presented in Fig. 3 for all the films. Although the elastic strain varies between samples, the relaxation of the films is above 90%, as estimated from the difference of the relaxed and measured lattice parameters, relative to the sub-

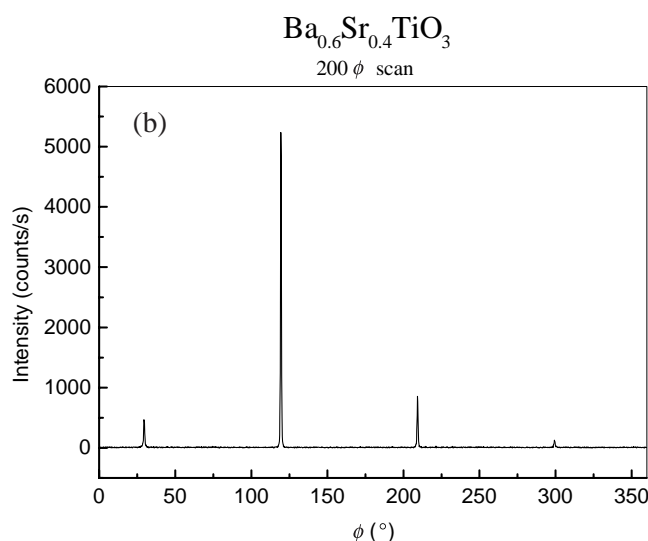
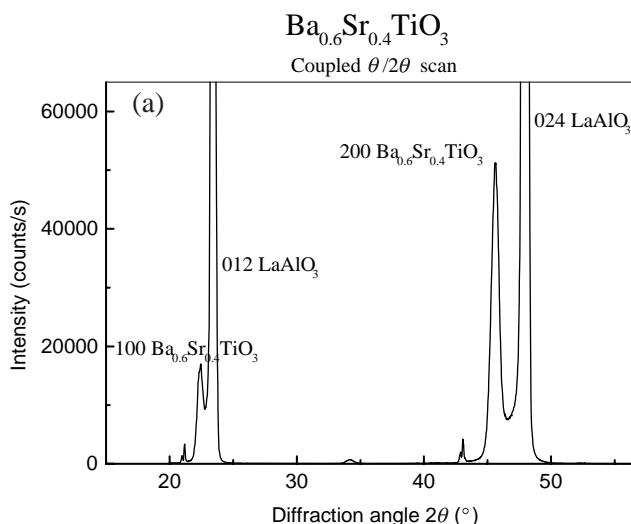


Fig. 2. X-ray diffraction scans of the undoped Ba_{0.60}Sr_{0.40}TiO₃ thin film on the LaAlO₃ substrate: (a) Perpendicular to the film surface; (b) Parallel to the film surface.

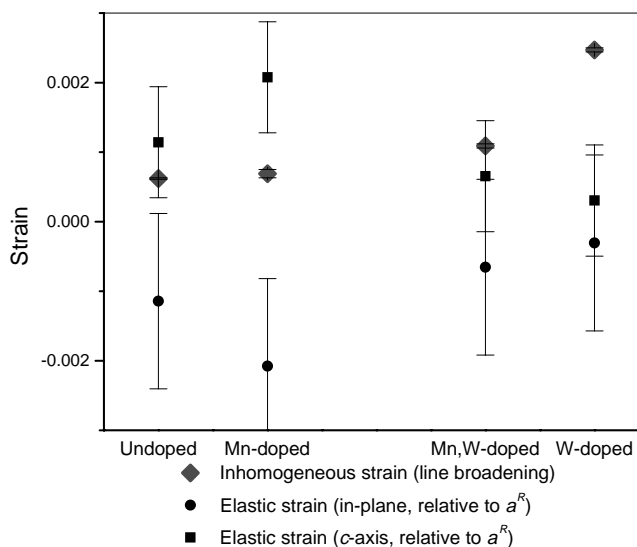


Fig. 3. Elastic and inhomogeneous strain for four thin films: undoped Ba_{0.60}Sr_{0.40}TiO₃, single-doped and co-doped Ba_{0.60}Sr_{0.40}Ti_{0.99}M_{0.01}O₃ (M = Mn, W). Error bars were estimated from the counting statistics of diffraction measurements through the propagation of errors.

strate lattice parameter a_s :

$$R = \frac{a - a_s}{a^R - a_s} 100.$$

The relaxation process is greatly dependent on the geometry of misfit dislocations and misfit between the film and substrate lattice parameter, which define the critical thickness for introduction of misfit dislocations. For this large a misfit, the critical thickness is estimated as being below 100 Å.¹⁶⁾ Because the thickness of both thin films was determined to be larger than 1000 Å by ellipsometry measurements, the relaxation should be complete at the growth temperature and any residual elastic strain should stem from differences in thermal expansion coefficients between the film and the substrate. However, because the doping at a 1% level cannot appreciably change thermal expansion coefficients, the difference in lattice parameters between the pristine and doped samples cannot be explained entirely by cooling effects. This might indicate that the doping influences the relaxation mechanism at the deposition temperature. The relaxation degree yields information about the linear density of misfit dislocations ρ_1

$$a/a_s - 1 = b\rho_1$$

where b is the magnitude of the Burger's vector. For all films, the misfit dislocation density is on the order of $10^6/\text{cm}$.

Threading dislocation densities, which do not affect lattice parameters, can be determined through the analysis of diffraction line breadths.¹⁷⁾ Generally, dislocations broaden diffraction lines of epitaxial thin films for three principal reasons: (i) dislocations define both twist (in-plane rotations) and tilt (perpendicular rotations) boundaries between grains; (ii) dislocations cause inhomogeneous strain fields and thus local changes in the d spacing and thus the additional line broadening; (iii) dislocation configurations may subdivide columnar grains into subgrain domains. Following the Ayers approach,¹⁸⁾ dislocation density due to (i) was estimated to about $8 \times 10^8/\text{cm}^2$, and it is approximately equal for all the samples, being somewhat different for the W-doped film (see Fig. 4). To estimate the effect of domain size according to (iii)

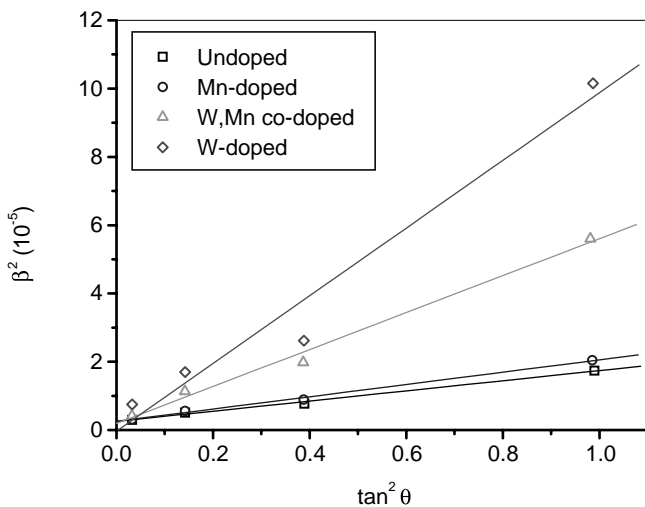


Fig. 4. The square of the integral breadth of the thin-film diffraction lines, corrected for the effects of instrumental broadening, as a function of $\tan^2 \theta$ for all four thin films. The intercept yields threading dislocation density and the slope inhomogeneous strain.

perpendicular to the film surface, we followed the broadening analysis formalism described elsewhere.¹⁴⁾ Domain size varies from 850–1550 Å and is close to the measured thickness of the films. The values differ because diffraction measures the dimension of grains perpendicular to the substrate and is therefore reduced because of grain tilts and possible extended defects parallel to the surface. The inhomogeneous-strain values resulting from (ii) are given in Fig. 3. There is a large increase in inhomogeneous strain for the co-doped but especially for the W-doped sample. It appears that the W doping on the Ti site strongly influences the defect concentration, either because the relaxation mechanism at growth temperature is affected, which would influence the dislocation density, or because the W doping affects the point defect concentration. There is a possibility that both effects are at work because the diffusion of point defects seems to be essential to the kinetic process of dislocation reactions, as showed for the BaTiO₃/SrTiO₃ system.¹⁹⁾ It is expected that doping with W on the Ti site should partially compensate oxygen vacancies, which would have an opposite effect on strain. However, at the same time, the doping might increase the density of Ti interstitials, which is then expected to increase inhomogeneous strain if interstitials are nonrandomly distributed at the preferential crystallographic sites. This point warrants a careful study of point defect concentration and distribution, which is the focus of the future study.

The difference in inhomogeneous strain is responsible for the relatively large contribution to the change of ferroelectric properties. Following eq. (2), in Fig. 5 we plot the shift of the Curie-Weiss temperature for both models, that is, when only elastic-strain contribution is considered, and when both elastic and inhomogeneous strain are taken into account. It is evident that the latter shows a much better correlation. Figure 3 indicates that the elastic and inhomogeneous strains are most often of a complementary magnitude. For instance, if a relief of elastic strain by introduction of misfit dislocations at the growth temperature was smaller, this would cause a larger

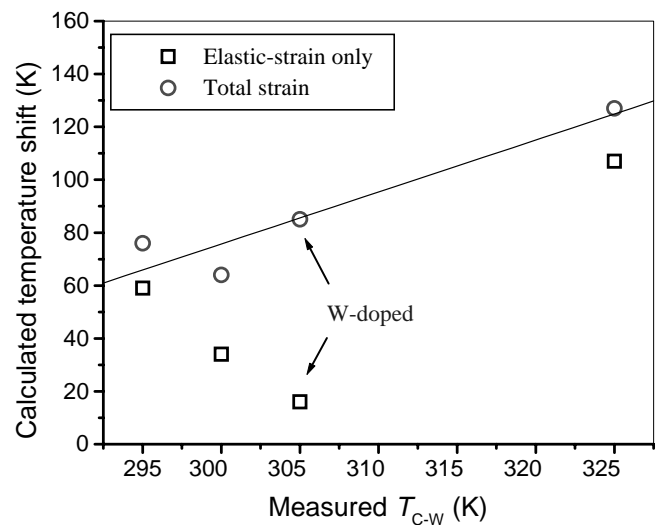


Fig. 5. Temperature shift of the Curie-Weiss temperature, calculated by eq. (2) for both elastic strain and total (elastic and inhomogeneous) strain contribution to the Gibbs free energy as a function of Curie-Weiss temperature determined from the dielectric measurements (compare Fig. 1). Note an especially large influence on the result for the W-doped film.

elastic strain in the lattice, and *vice versa*. This implies that minimizing dielectric loss through the relief of only elastic strains might not yield the desired effect because the total strain, that is both elastic and defect-related inhomogeneous strain, should rather be used to estimate effects on the ferroelectric and dielectric properties of thin films.

5. Conclusions

The results indicate that the doping at Ti site influences the microstructure of BSTO epitaxial thin films grown on the (001) LAO substrate. The misfit relaxation is suppressed in the case of Mn but increases when doping with W. Both compressive in-plane elastic strains (stresses) and in particular inhomogeneous strains influence the observed increase in Curie-Weiss temperature. This seems to corroborate the assumption that the Curie-Weiss temperature and extrinsic dielectric losses strongly depend on internal stresses and defects. For a good agreement with the thermodynamic theory, it is necessary to consider the contribution of inhomogeneous strains.

- 1) O. Auciello, J. F. Scott and R. Ramesh: Phys. Today **51** (1998) 22.
- 2) A. M. Hermann, J. C. Price, J. F. Scott, R. M. Yandrofski, A. Naziripour, D. Galt, H. M. Duan, M. Paranthaman, R. Tello, J. Cuchiaro and R. K. Ahrenkiel: Bull. Am. Phys. Soc. **38** (1993) 689.
- 3) W. Chang, J. S. Horwitz, A. C. Carter, J. M. Pond, S. W. Kirchoefer, C. M. Gilmore and D. B. Chrisey: Appl. Phys. Lett. **74** (1999) 1033.
- 4) H.-C. Li, W. Si, A. D. West and X. X. Xi: Appl. Phys. Lett. **73** (1998) 464.
- 5) M. J. Dalberth, J. C. Price and C. T. Rogers: Ferroelectric Thin Films VI Symp., Mater. Res. Soc., 1998, p. 371.
- 6) H.-C. Li, W. Si, R.-L. Wang, Y. Xuan, B.-T. Liu and X. X. Xi: Mater. Sci. Eng. **B56** (1998) 218.
- 7) W. Chang, J. S. Horwitz, W. J. Kim, J. M. Pond, S. W. Kirchoefer, C. M. Gilmore, S. B. Qadri and D. B. Chrisey: Mater. Res. Soc. Symp. **541** (1999) 693.
- 8) W. Chang, J. S. Horwitz, W. J. Kim, J. M. Pond, S. W. Kirchoefer and D. B. Chrisey: Mater. Res. Soc. Symp. **541** (1999) 699.
- 9) A. M. Hermann, V. Badri, P. A. Ramakrishnan and D. Balzar: to be published in Integr. Ferroelectr.
- 10) N. A. Pertsev, A. G. Zembilgotov and A. K. Tagantsev: Phys. Rev. Lett. **80** (1998) 1988.
- 11) M. E. Lines and A. M. Glass: *Principles and Applications of Ferroelectrics and Related Materials* (Clarendon Press, Oxford, 2001) p. 112.
- 12) D. Balzar, P. A. Ramakrishnan and A. M. Hermann: to be published in Appl. Phys. Lett.
- 13) Commercial brand names are given for identification purpose only.
- 14) D. Balzar: in *Defect and Microstructure Analysis by Diffraction*, eds. R. L. Snyder, H. J. Bunge and J. Fiala, International Union of Crystallography Monographs on Crystallography No. 10 (Oxford University Press, New York, 1999) p. 94.
- 15) Card # 34-0411, Powder Diffraction File, ICDD, Pennsylvania.
- 16) J. S. Speck and W. Pompe: J. Appl. Phys. **76** (1994) 466.
- 17) M. J. Hordon and B. L. Averbach: Acta Metall. **9** (1961) 237.
- 18) J. E. Ayers: J. Cryst. Growth **135** (1994) 71.
- 19) T. Suzuki, Y. Nishi and M. Fujimoto: Philos. Mag. **A 79** (1999) 2461.